

Selective Functionalization of the Outer and Inner Surfaces in Mesoporous Silica Nanoparticles

Johann Kecht, Axel Schlossbauer, and Thomas Bein*

Department of Chemistry and Biochemistry and Center for NanoScience (CeNS), University of Munich (LMU), Butenandtstr. 11 (E), 81377 Munich, Germany

Received June 1, 2008. Revised Manuscript Received July 8, 2008

The site-selective functionalization of mesoporous nanoparticles was achieved with a sequential co-condensation approach. Using this strategy, functional groups were completely dispersed inside the channels, concentrated in parts of the mesopores, or exclusively placed on the external surface of colloidal mesoporous silica nanoparticles depending on the time of addition of the desired functionality. This method overcomes some of the inherent disadvantages often found in selective functionalization by grafting approaches, that is, partial diffusion of reactant species inside the channels and the lack of control over the amount of incorporated organic moieties. Furthermore, the functional group density on the outer particle surface can be easily adjusted by variation of the organosilane-to-silane ratio.

Introduction

Mesoporous structured materials have attracted a great deal of interest in recent years due to their ordered porosity and high internal surface area.^{1,2} If additional molecular functionality can be introduced in a controlled way, it is possible to adjust many key properties, including hydrothermal stability, surface polarity, and the density of attached organic moieties, which are crucial for applications in sorption, catalysis, templating, and host–guest chemistry.^{3,4} Within these growing fields, new advanced applications begin to emerge that require more sophisticated materials, that is, drug delivery systems with multiple functionalities.^{5,6} Thus, the selective functionalization of specific locations inside mesoporous materials becomes a point of interest to gain greater control over the surface properties.

A recent example of such work includes the separate functionalization of the inner surface in micropores and mesopores of SBA-15 silica.⁷ By partial cleavage of the P123 surfactant, the mesopore surface could be functionalized with trimethylchlorosilane while the micropores remained inac-

cessible until a subsequent heating treatment removed the remaining surfactant. The micropore surface was then functionalized with trivinylchlorosilane and reacted with a palladium complex to generate a final product with fully accessible mesopores and Pd nanoparticles located inside the micropores.

Other examples of site-selective functionalization include the generation of Janus particles, in which the surfaces located on both hemispheres of a round particle are of different types.⁸ Such particles were produced from nonporous fused silica spheres with diameters of 800 nm and 1.5 μm , respectively. The selectivity was achieved by fixating the particles at the liquid–liquid interface of emulsified molten wax in water, followed by solidification of the wax and subsequent functionalization of the half-embedded silica.⁹ This approach allowed production of bipolar (cationic–anionic) and surfactant-like (cationic–hydrophobic) silica Janus particles in gram-scale quantities.

Recent investigations center on the selective functionalization of the outer and inner surface in mesoporous silica systems.^{10–12} These locations are especially relevant for mesoporous silica nanoparticles with sizes below 100 nm, which possess a high external surface area in addition to the inner surface of the mesopores. Mesoporous silica nanoparticles can be prepared as stable colloidal suspensions and can subsequently be used for the construction of hierarchical

* Corresponding author. Fax: (+) 49 89 218077622. Tel: (+) 49 89 218077623. E-mail: bein@lmu.de.

- (1) Hoffmann, F.; Cornelius, M.; Morell, J.; Froeba, M. *Angew. Chem., Int. Ed.* **2006**, *45*, 3216–3251.
- (2) Wan, Y.; Zhao, D. *Chem. Rev.* **2007**, *107*, 2821–60.
- (3) Ford, D. M.; Simanek, E. E.; Shantz, D. F. *Nanotechnology* **2005**, *16*, 458–475.
- (4) Stein, A.; Melde, B. J.; Schroden, R. C. *Adv. Mater.* **2000**, *12*, 1403–1419.
- (5) Slowing, I. I.; Trewyn, B. G.; Giri, S.; Lin, V. S. Y. *Adv. Funct. Mater.* **2007**, *17*, 1225–1236.
- (6) Giri, S.; Trewyn, B. G.; Lin, V. S. Y. *Nanomedicine* **2007**, *2*, 99–111.
- (7) Yang, C.-M.; Lin, H.-A.; Zibrowius, B.; Spliethoff, B.; Schueth, F.; Liou, S.-C.; Chu, M. W.; Chen, C.-H. *Chem. Mater.* **2007**, *19*, 3205–3211.

- (8) Perro, A.; Reculusa, S.; Ravaine, S.; Bourgeat-Lami, E.; Duguet, E. *J. Mater. Chem.* **2005**, *15*, 3745–3760.

- (9) Hong, L.; Jiang, S.; Granick, S. *Langmuir* **2006**, *22*, 9495–9499.

- (10) Shephard, D. S.; Zhou, W.; Maschmeyer, T.; Matters, J. M.; Roper, C. L.; Parsons, S.; Johnson, B. F. G.; Duer, M. J. *Angew. Chem., Int. Ed.* **1998**, *37*, 2719–2723.

- (11) De Juan, F.; Ruiz-Hitzky, E. *Adv. Mater.* **2000**, *12*, 430–432.

- (12) Cheng, K.; Landry, C. C. *J. Am. Chem. Soc.* **2007**, *129*, 9674–9685.

porous materials and thin films, thus offering many possibilities for new applications in research fields such as sensing, optics, and drug delivery.^{5,13} Functionalization of the external nanoparticle surface is of paramount importance for colloidal stability and interaction with the environment, that is, with living cells and other biological substrates, and allows the attachment of large molecular moieties and nanoscale building blocks without reducing pore size and available free pore volume. On the other hand, functionalization of the internal pore system is needed to control and fine-tune the host–guest chemistry, that is, for drug delivery, catalysis, and sorption applications.

Recently, Fmoc (9-fluorenylmethyloxycarbonyl) protected alkylamines grafted on mesoporous silica spheres were differentially functionalized by diffusion-based cleavage with piperidine solution.¹² Moreover, it was shown that during grafting reactions the external surface is more accessible and grafted preferentially to the inner pore system even in empty calcined MCM-41.¹⁰ Functional groups deposited at the channel opening may also slow down the diffusion of further grafting reagents, thus resulting in an inhomogeneous distribution of attached groups.¹⁴ Similar results were obtained for template-filled as-synthesized MCM-41 which upon exposure to trimethylsilylchloride was functionalized mainly on the external surface.¹¹ However, several publications demonstrate that grafting reagents including various chloro- and trialkoxysilanes can easily and efficiently enter the template-filled channels and functionalize the inner pore systems, in some cases even producing extracted materials by completely replacing the surfactant molecules.^{15–18} In fact, results of the present work reveal that functionalization inside template-filled pores already occurs at very mild conditions, that is, after reaction for 4 h at room temperature.

In view of these challenges we present a new approach for the highly selective control of the outer versus the internal pore surface in colloidal mesoporous silica nanoparticles. By using a site-selective co-condensation approach, the particle is functionalized in situ either during or after the growth process. In comparison to grafting approaches, much greater control over the amount and density of the functional groups is achieved. By choosing suitable reaction conditions, unwanted functionalization of the inner pore surface can be completely inhibited. Furthermore, functionalization by co-condensation is known to produce a more homogeneous surface functionalization than grafting.

Experimental Section

Reagents. Tetraethyl orthosilicate (TEOS, Fluka, >98%), ammonia (Aldrich, 25% in H₂O) phenyltriethoxysilane (PTES, Aldrich, 98%), aminopropyltriethoxysilane (APTES, ABCR, 96%), 11-bromo-undecyltrimethoxysilane (BUTMS, ABCR, 95%), cetyltri-

Table 1. Samples Functionalized by Post-Synthesis Grafting of Template-Containing Mesoporous Silica and Subsequent Extraction of the Template

sample name	material	grafting agent (RTES)	reaction temperature
Ph-MS 1	MCM-41	PTES	25 °C
Ph-MS 2	MCM-41	PTES	reflux
AP-MS 3	MCM-41	APTES	25 °C
BU-MS 4	MCM-41	BUTMS	25 °C
Ph-CMS 5	CMS	PTES	25 °C
AP-CMS 6	CMS	APTES	25 °C

methylammonium bromide (CTAB, Aldrich, 95%), cetyltrimethylammonium chloride (CTAC, Fluka, 25% in H₂O), and triethanolamine (TEA, Aldrich, 98%) were used as received without further purification. Doubly distilled water from a Millipore system (Milli-Q Academic A10) was used for all synthesis and purification steps.

Preparation of Micrometer-Sized MCM-41 Particles. MCM-41 was prepared according to a published procedure.¹⁹ To a stirred solution of CTAB (2.39 g, 6.56 mmol), water (125 g, 6.94 mol), ethanol (12.5 g, 271 mmol), and aqueous ammonia (25 wt %, 9.18 g, 135 mmol) in a 300 mL polypropylene reactor, the amount of 10.0 g of TEOS (48.2 mmol) was added. The resulting mixture has a molar composition of 1 TEOS:0.14 CTAB:144 H₂O:5.63 ethanol:2.8 NH₃. After stirring for 2 h at room temperature, the reaction mixture was filtered off and washed with 50 mL of water. The resulting white powder was dried at 60 °C for 12 h.

Preparation of Colloidal Mesoporous Silica (CMS) Nanoparticles. Mesoporous silica nanoparticles were prepared according to ref 20 from reaction mixtures with a molar composition of 1 TEOS:0.20 CTAC:10.37 TEA:130.2 H₂O. The combined TEOS (1.92 g, 9.22 mmol) and TEA (14.3 g, 95.6 mmol) were heated for 20 min at 90 °C without stirring in a 100 mL polypropylene reactor. A solution of CTAC (25% in water, 2.41 mL, 1.83 mmol) and water (21.7 g, 1.21 mol) preheated to 60 °C was added, and the resulting mixture was stirred at room temperature for 12 h. After addition of 100 mL of ethanol, the mesoporous silica nanoparticles were separated by centrifugation and redispersed in ethanol.

General Procedure for the Selective Functionalization by Grafting of Template-Containing MCM-41. As-synthesized MCM-41 (360 mg) was added to dry toluene (5 mL) in a dry flask under nitrogen atmosphere. After addition of 1 mmol of the respective functionalized trialkoxysilane, the reaction mixture was stirred for 4 h at room temperature or under reflux conditions (see Table 1). The functionalized MCM-41 was filtered off and washed with 20 mL each of toluene, methanol, and water before being exposed to the MCM-41 extraction procedure. In the case of CMS materials, the grafting was performed by direct reaction of the ethanolic suspensions (~3 wt %) with the triethoxysilanes and purification of the resulting suspensions via multistep centrifugation (see Table 1).

General Procedure for the Selective Functionalization of CMS by Co-Condensation. The reactants were mixed following the synthesis procedure for CMS. However, a second set of reactants was added at specific time periods after combination of the initial TEOS/TEA and CTAC solutions (see Table 2). The reactants were added to the stirred reaction mixture with an Eppendorf micropipette and consist of TEOS and a functionalized triethoxysilane (RTES) in varying ratios. The combined amount of both silanes was 185 μmol in all samples, that is, 2% of the total amount of “Si” in the initial CMS synthesis. The resulting mixture was stirred at room temperature for 12 h followed by purification and extraction as described for CMS.

(13) Lin, Y.-S.; Wu, S.-H.; Hung, Y.; Chou, Y.-H.; Chang, C.; Lin, M.-L.; Tsai, C.-P.; Mou, C.-Y. *Chem. Mater.* **2006**, *18*, 5170–5172.

(14) Lim, M. H.; Stein, A. *Chem. Mater.* **1999**, *11*, 3285–3295.

(15) Bourlinos, A. B.; Karakostas, T.; Petridis, D. *J. Phys. Chem. B* **2003**, *107*, 920–925.

(16) Antochshuk, V.; Jaroniec, M. *Chem. Commun.* **1999**, 2373–2374.

(17) Antochshuk, V.; Jaroniec, M. *Chem. Mater.* **2000**, *12*, 2496–2501.

(18) Antochshuk, V.; Araujo, A. S.; Jaroniec, M. *J. Phys. Chem. B* **2000**, *104*, 9713–9719.

(19) Grun, M.; Unger, K. K.; Matsumoto, A.; Tsutsumi, K. *Microporous Mesoporous Mater.* **1999**, *27*, 207–216.

Table 2. Samples Obtained via in Situ Functionalization by Co-Condensation

sample name	triethoxysilane (RTES)	TEOS:RTES relative molar ratio ^a	TEOS:RTES volumes [$\mu\text{L}:\mu\text{L}$]	addition time [min]
AP-CMS 7	APTES	0.5:0.5	20.5:21.5	5
AP-CMS 8	APTES	0.5:0.5	20.5:21.5	10
AP-CMS 9	APTES	0.5:0.5	20.5:21.5	30
AP-CMS 10	APTES	0.5:0.5	20.5:21.5	60
AP-CMS 11	APTES	0:1	0:43.0	30
AP-CMS 12	APTES	0.8:0.2	32.8:8.6	30
AP-CMS 13	APTES	0.95:0.05	39.25:2.1	30
Ph-CMS 14	PTES	0.5:0.5	20.5:22.3	30
Ph-CMS 15	PTES	0:1	0:44.6	30

^a Total silane amount = 185 μmol .

Extraction of MCM-41 and CMS. Extraction of the organic template from the MCM-41 and CMS materials was performed by heating 1 g twice under reflux at 90 °C for 30 min in a solution containing 2 g of ammonium nitrate in 100 mL of ethanol, followed by 30 min under reflux in a solution of 4 g of concentrated hydrochloric acid in 100 mL of ethanol. The MCM-41 material was separated by filtration, and the CMS nanoparticles were purified by centrifugation. Both types of materials were washed with ethanol after each extraction step. MCM-41 and CMS materials were obtained as white solid powders and as clear ethanolic suspensions, respectively.

Characterization. Dynamic light scattering (DLS) and zeta potential measurements were performed on a Malvern Zetasizer-Nano instrument equipped with a 4 mW He-Ne laser (633 nm) and avalanche photodiode detector. DLS measurements were directly recorded in ethanolic colloidal suspensions. For determination of the zeta potential curves, one drop of the ethanolic suspension (~3 wt %) was mixed with 1 mL of commercial Hydron Buffer solution of the appropriate pH prior to measurement. This approach allowed fast and reproducible zeta potential measurements which are comparable to the respective curves obtained by pH adjustment via addition of hydrochloric acid (see Supporting Information Figure SI-1). Thermogravimetric analyses (TGA) of the bulk samples were performed on a Netzsch STA 440 C TG/DSC (heating rate of 10 K/min in a stream of synthetic air of about 25 mL/min). Raman spectra were recorded on a Jobin Yvon Horiba HR800 UV Raman microscope using a HeNe laser emitting at 632.8 nm. IR spectra were recorded on a Bruker Equinox 55 under diffuse reflectance conditions (samples were mixed with KBr, and spectra are background subtracted). Scanning transmission electron microscopy (STEM) was performed on a Titan 80–300 kV microscope operating at 300 kV equipped with a high-angle annular dark field detector. STEM samples stained with iridium were prepared by adding three drops of an aqueous 1 M solution of IrCl_3 to 3 mL of an ethanolic/aqueous CMS suspension (~3 wt %), followed by two steps of centrifugation, washing with ethanol, and subsequent drying of a drop of the resulting diluted colloidal suspension on a carbon-coated copper grid. During TEM studies, it was observed that the clustered iridium atoms did not change location and size even after prolonged exposure to the TEM beam. As a result of the spherical shape of the CMS particles, higher background intensities are observed near the particle centers because of the increased thickness of the silica material traversed by the electron beam. Analysis of the micrographs was therefore performed in multiple steps by adjusting brightness and contrast for different ranges of radii in each CMS particle to account for all iridium clusters. Nitrogen sorption measurements were performed on a Quantachrome Instruments NOVA 4000e at 77 K. For calculations of pore sizes and volumes a non-local density functional theory (NLDFT) equilibrium model of N_2 on silica was used. The BET model was applied to evaluate the surface areas.

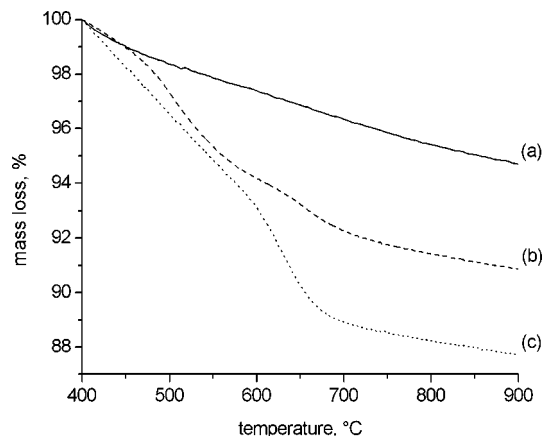


Figure 1. Thermogravimetric data for unfunctionalized MCM-41 (a) and phenyl-functionalized samples Ph-MS 1 (b) and Ph-MS 2 (c).

Results and Discussion

To selectively functionalize the inner and outer surface of mesoporous silica nanoparticles, two different approaches based on grafting and co-condensation reactions were investigated and compared.

The first approach is based on the grafting of template-containing mesoporous materials. Micrometer-sized MCM-41 type silica particles were employed as a model system with a high ratio of inner to outer surface. By performing the grafting while the mesopore channels are occupied by template molecules, diffusion of the grafting reactant into the porous structure is limited, thus leading to a preferential functionalization of the outer particle surface. As-synthesized samples were grafted with phenyltriethoxysilane (PTES) and aminopropyltriethoxysilane (APTES) at different temperatures before extraction of the organic template (see Table 1). After the grafting procedure, the template was removed by extraction prior to further characterization. Thermogravimetric analysis was performed to determine the amount of incorporated phenyl groups (Figure 1).

As a result of the thermal stability of the aromatic ring, combustion of grafted phenyl occurs at elevated temperatures over 400 °C, in contrast to most aliphatic groups which decompose in a temperature range between 110 and 400 °C.²¹ Extracted mesoporous silica without additional grafting shows only a minor weight loss over 400 °C which can be attributed to silanol condensation (Figure 1a). Template-containing materials grafted with PTES at room temperature and under reflux conditions display a significantly higher weight loss in this temperature range due to the incorporated phenyl groups (Figure 1b,c; TG data for the temperature range 25–900 °C can be found in the Supporting Information Figure SI-2). As can be seen, the phenyl content inside the mesoporous materials strongly depends on the grafting temperature, and a lower amount is incorporated at room temperature as compared to reflux conditions. These observations were confirmed by nitrogen sorption. Correspondingly, samples with higher phenyl contents in TGA display

(20) Möller, K.; Kobler, J.; Bein, T. *Adv. Funct. Mater.* **2007**, *17*, 605–612.

(21) Kleitz, F.; Schmidt, W.; Schuth, F. *Microporous Mesoporous Mater.* **2003**, *65*, 1–29.

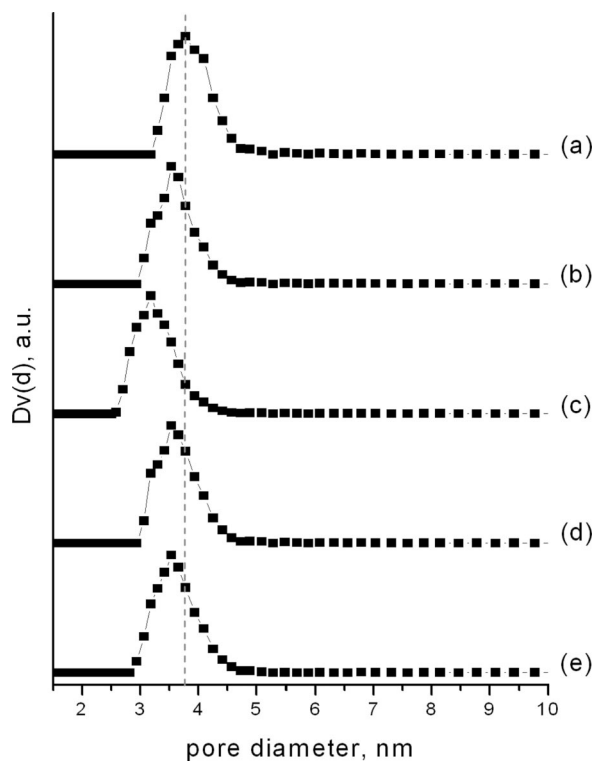


Figure 2. Pore diameters derived from nitrogen sorption isotherms of unfunctionalized MCM-41 (a) and samples Ph-MS 1 (b), Ph-MS 2 (c), AP-MS 3 (d), and BU-MS 4 (e).

smaller pore diameters (Figure 2; for the corresponding isotherms, surface areas, and pore volumes see Supporting Information Figure SI-3 and Table SI-1). However, a minor reduction of the pore diameter is observed in samples obtained by grafting of template-containing materials even at mild conditions (Figure 2).

It can therefore be concluded that 4 h at room temperature is sufficient to at least partially functionalize the inside of the filled mesopores and that at higher temperatures it is possible to replace a major part of the template with the grafting reagent. Similar observations were made for template-containing MCM-41 grafted with APTES and BUTMS (Figure 2) and for colloidal mesoporous silica (CMS) samples grafted with APTES and PTES (see Supporting Information Figure SI-4). In case of the nanoscale particles with shorter diffusion paths, the functionalization by expulsion of template molecules can be observed even more clearly, especially by grafting with APTES. The presence of the corresponding organic moieties in the materials was also confirmed by Raman spectroscopy (see Supporting Information Figure SI-5).

Occluded template slows the diffusion of the grafting reactant into the pores, therefore favoring the preferential functionalization at the outer surface. As demonstrated above, diffusion into the pores can be further limited by lowering the grafting temperature. However, even at mild conditions a small part of the reactants diffuse into the structure and functionalize the inner pore surface to a significant degree. This behavior is problematic for certain applications; for example, the attachment of large moieties is not possible without causing pore blocking. Furthermore, a precise control

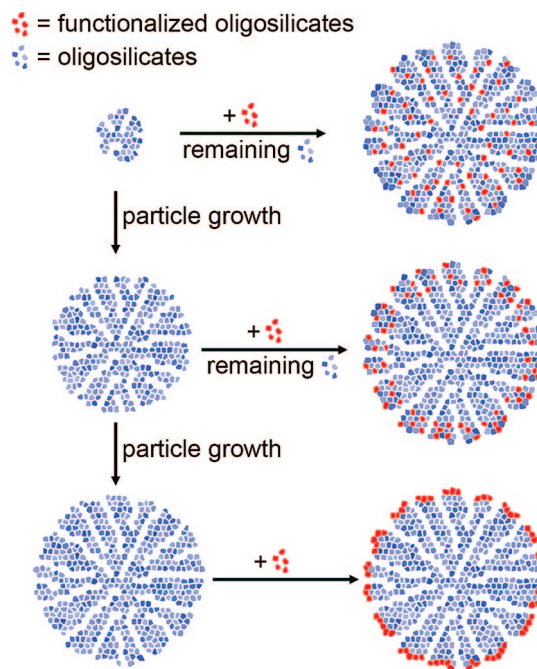


Figure 3. Distribution of functional groups depending on the addition time of the organosilane component during synthesis.

over the amount and location of functional groups is not possible by this grafting-based method.

In our novel approach addressing these issues, colloidal mesoporous silica (CMS) nanoparticles were functionalized in situ during their growth process by site-selective co-condensation instead of postsynthesis grafting.

CMS materials were synthesized according to our previously published procedures.²⁰ TEOS was hydrolyzed in a reaction mixture containing CTAC and triethanolamine, resulting in high nucleation rates and slow subsequent growth of the generated seeds. By using this method, stable ethanolic suspensions of mesoporous nanoparticles with sizes below 100 nm were obtained after extraction. Co-condensed CMS can be obtained by incorporation of organosilanes in the batch composition as described in previous studies.²²

By the addition of small amounts (2 mol % of total silane content) of a mixture of functionalized triethoxysilanes (RTES) and TEOS at specific times during synthesis, it is possible to control the location of the organic moieties. Depending on the addition time, the functionalized groups are either dispersed more homogeneously throughout the particle or concentrated inside a shell in the outer regions (Figure 3).

As demonstrated in the following, the concentration of functional groups on the external surface increases at later addition times due to particle growth. If the addition takes place after complete growth of the particle, the functionalized silanes condense only on the last layer, that is, on the outer particle surface.

To monitor this change in density of functional groups on the external surface, zeta potential measurements were performed at pH values between 2 and 6 on samples prepared by addition of an APTES/TEOS mixture (molar ratio 1:1)

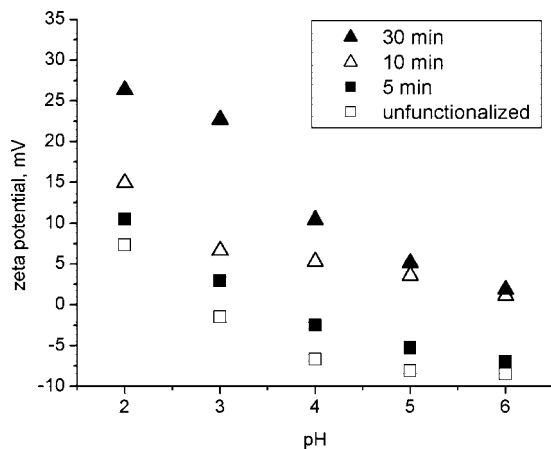


Figure 4. Zeta potential of samples prepared by variation of the addition time of the APTES/TEOS mixture: samples AP-CMS 9 (filled triangles), AP-CMS 8 (empty triangles), AP-CMS 7 (filled squares), and unfunctionalized CMS (empty squares).

at different stages of particle growth (Figure 4). The use of zeta potential measurements for the determination of the amount and location of amine functionalities in mesoporous silica has been reported in the literature.^{23,24}

The incorporated aminopropyl moieties are protonated at acidic pH values and carry a positive charge. A higher density of such groups on the outer particle layer thus leads to increased zeta potential curves as they affect the overall surface charge. Conversely, functional groups located at the interior surface, that is, the channel walls of the mesopores, do not contribute to the zeta potential.

As can be seen, the zeta potential and thus the concentration of aminopropyl groups on the outer surface is strongly dependent upon the time of addition. Early APTES/TEOS addition, for example, after 5 min, only leads to a minor increase of the zeta potential curve as the organic groups are dispersed throughout a large volume of the particle and only a few are located on the external surface. However, addition of the same APTES/TEOS amount at later times, that is, after 10 and 30 min, generates more positive surface charges (Figure 4). Interestingly, increasing the addition time above 30 min does not lead to significantly higher zeta potentials, as the particles are fully grown at this point (see Supporting Information Figure SI-6). The observed zeta potential obtained after an addition delay of 30 min is about half that of a completely APTES-saturated surface. This observation is in accordance with the employed APTES/TEOS ratio of 1:1 and proves the high concentration of positively charged functional groups at the outer interface. Despite the small amounts of employed organosilane (2%), the organosilane groups are concentrated at the densely functionalized outer surface. The outer layer thus possesses a high positive charge at low pH values, which is only partially compensated by the negative charge of the silanol groups.

Transmission electron microscopy was performed as a complementary approach for determining the location of the

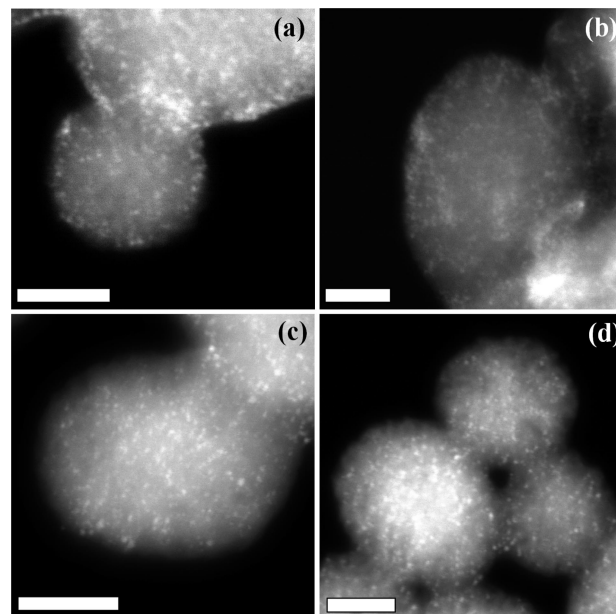


Figure 5. STEM micrographs of samples AP-CMS 9 (a, b) and AP-CMS 8 (c, d) (scale bar = 20 nm).

aminopropyl groups in the mesoporous silica nanoparticles. To distinguish between functionalized and unfunctionalized surfaces, iridium(III) chloride was added as a contrast agent and uncomplexed iridium cations were removed by two steps of washing and centrifugation. Control studies showed that iridium does not adhere to unfunctionalized silica surfaces at the given conditions and is removed in the first washing step. STEM (scanning transmission electron microscopy) was performed to visualize the heavy metal content in the stained CMS particles of samples prepared with addition times of 10 min (AP-CMS 8) and 30 min (AP-CMS 9), respectively (Figure 5).

This technique allows *Z*-contrast imaging with an intensity proportional to Z^2 , the squared atomic number of the elements present, resulting in clearly visible bright spots corresponding to clustered heavy iridium atoms. As STEM shows a two-dimensional projection, these spots are positioned over the whole imaged particle but with different radial distributions depending on the location of the functional groups. Depending on the addition time in the selective functionalization procedure, the resulting materials can attain any state between two extreme cases; that is, either the aminopropyl groups and thus the iridium clusters are homogeneously distributed over the whole particle volume, or they are solely located on the outer particle surface. For statistical analysis each investigated particle was divided into two segments corresponding to equal volumes transmitted by the electron beam, that is, an “inner part” and “outer part”, by placing a circle or ellipsoid with a relative diameter of 60.8% in the center of each particle projection (see Figure 6a).

The corresponding volumes transmitted by the electron beam in both areas are equal, and thus the number distribution of iridium clusters in those two areas is expected to be 1:1 in the case of a homogeneous distribution over the whole particle volume (assuming similar nucleation and growth rates for the clusters throughout the particles). On the other hand, a relative distribution of 0.642:1 for the inner and outer

(23) Rosenholm, J. M.; Linden, M. *Chem. Mater.* **2007**, *19*, 5023–5034.

(24) Rosenholm, J. M.; Duchanoy, A.; Linden, M. *Chem. Mater.* **2008**, *20*, 1126–1133.

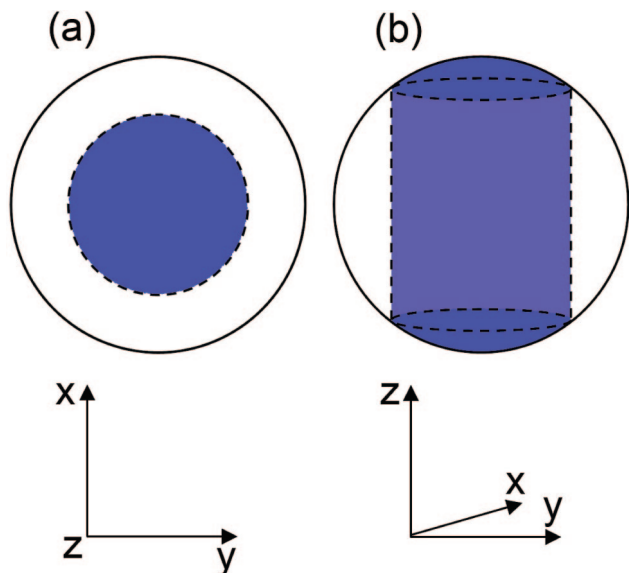


Figure 6. Scheme of a CMS particle divided into the “inner part” (darkened area) and “outer part” (white area) seen along the z -axis parallel to the STEM electron beam (a). The same particle oriented sideways shows the corresponding volumes transmitted by the STEM electron beam (b).

parts is expected if iridium clusters are present solely on the external surface, that is, the ratio corresponding to the external particle surfaces traversed by the electron beam (for detailed calculations please refer to the Supporting Information Figure SI-7). While it is expected that the organosilanes were completely incorporated in both samples during co-condensation based on the obtained data, it should be noted that these calculations are still valid even for different total amounts of functional groups. The calculated distribution values are relative ratios of the number of clusters in two volume parts of each particle and thus independent of the total amount of functional groups in each sample. A total of 1568 iridium clusters in 19 different CMS particles of both samples were evaluated, yielding a relative distribution and standard deviation of 0.986 ± 0.097 in sample AP-CMS **8** and 0.636 ± 0.045 in sample AP-CMS **9**. Both values are in good accordance with the calculated theoretical results for a selective functionalization of the external surface and a more homogeneous distribution inside the particle channels (assuming similar nucleation and growth rates for the clusters throughout the particles) and thus support the observations made by zeta potential measurements.

Using this selective co-condensation approach, a phenyl-functionalized sample (Ph-CMS **14**) was prepared by addition of a PTES/TEOS mixture with a molar ratio of 1:1 after 30 min. The presence of the attached functional groups in the externally functionalized silica material was shown by Raman spectroscopy (see Supporting Information Figure SI-8).

Nitrogen sorption measurements were performed to investigate the impact of the introduced functional groups on the porous network. As expected, no pore size reduction was observed in the externally functionalized samples (Figure 7, for the corresponding isotherms, BET surface areas, and pore volumes see Supporting Information Figure SI-9 and Table SI-2).

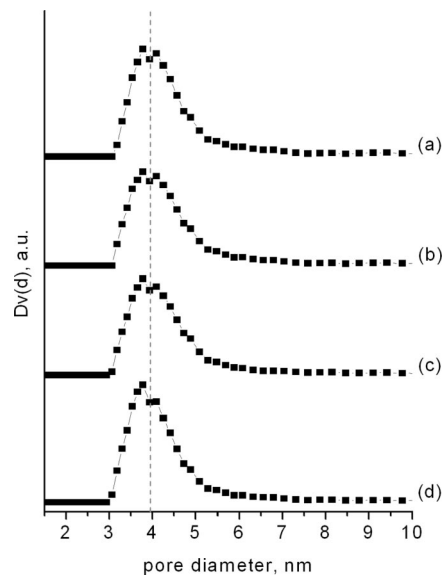


Figure 7. Pore diameters derived from nitrogen sorption isotherms of unfunctionalized CMS (a) and samples AP-CMS **9** (b), AP-CMS **8** (c), and Ph-CMS **14** (d).

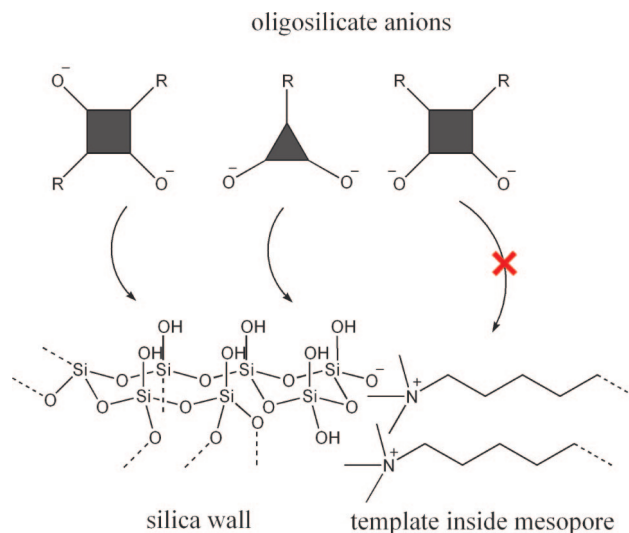


Figure 8. Formation mechanism of the outer layer during external functionalization of the mesoporous particle. Oligomeric organosilicate anions condense with the silica framework but cannot enter the hydrophobic interior of the micellar structure.

However, it should be noted that these data do not provide clear evidence for the location of the functional groups considering the small amounts of incorporated organosilane. As a result of the high internal surface area of the mesopores, dispersed groups cannot significantly influence the pore size due to their small concentration on the channel walls. However, the presence and location of these dispersed functional groups can be determined by combined zeta potential and STEM measurements even at very low concentrations, as has been demonstrated.

We propose a site-selective co-condensation mechanism for our new approach (see Figures 3 and 8).

The generation of mesoporous silica by hydrolysis of alkoxy silanes proceeds via formation of small anionic oligosilicates, which subsequently build up the inorganic framework by cooperative self-assembly with the surfactant

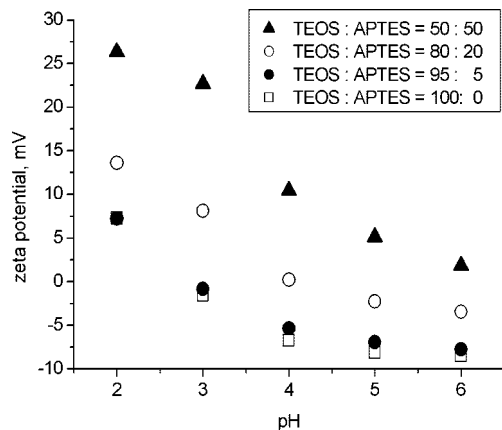


Figure 9. Zeta potential of samples with different APTES/TEOS ratios: samples AP-CMS 9 (filled triangles), AP-CMS 12 (empty circles), AP-CMS 13 (filled circles), and unfunctionalized CMS (empty squares).

micelles.^{25,26} As the organic moieties are introduced by in situ co-condensation in aqueous basic media ($\text{pH} > 9$), the trialkoxysilanes are rapidly hydrolyzed to give anionic species. This prevents entry into the nonpolar interior of the micelles inside the channels and subsequent exchange of template molecules, as observed for grafted nanoscale CMS (Figure 8). In this way, a locally selective functionalization becomes possible by co-condensation of the oligosilicates during framework formation of the growing particle. Depending on the time of addition of the organosilanes, three cases can be distinguished. A, the entire channel wall is functionalized in a classic co-condensation reaction; B, a part of the mesopore channels is functionalized during growth from an initially formed nucleus; or C, the oligosilicates attach themselves on the last layer of the outer surface of a fully grown particle.

Apart from allowing a precise control over the location of the functionalized groups, this co-condensation strategy also offers further advantages. Grafting methods are generally faced with the difficulty to accurately adjust functionalization density due to the various controlling factors such as reaction time, temperature, and reactant species, which determine the surface concentration of attached groups. However, by variation of the silane ratios in a co-condensation reaction it is possible to control the amount of incorporated groups. This was shown by zeta potential measurements of samples functionalized by aminopropyl on the outer particle surface. Samples AP-CMS 9, 11, 12, and 13 were prepared by addition of a silane mixture with different APTES/TEOS ratios after 30 min of particle growth. As can be seen, increasing amounts of incorporated aminopropyl groups lead to higher positive surface charges, thus demonstrating the successful adjustment of organic group densities on the particle surface (Figure 9).

However, a contrasting behavior is observed at very high ratios, that is, addition of the pure functionalized organosilane without additional TEOS in samples AP-CMS 11 and Ph-CMS 15: In the case of pure APTES, the recorded zeta potential curves of AP-CMS 11 showed a lower surface charge than samples prepared with a 1:1 mixture of APTES

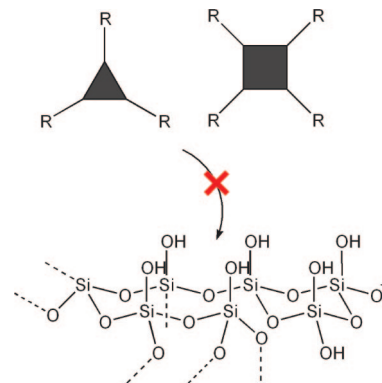


Figure 10. Organosilane oligomers lacking free silanol groups cannot condense with the silica framework during the external functionalization step.

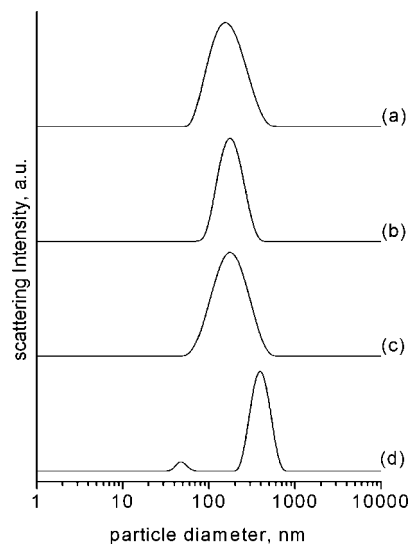


Figure 11. Unweighted DLS curves for ethanolic suspensions of unfunctionalized CMS (a) and samples Ph-CMS 14 (b), AP-CMS 9 (c), and AP-CMS 11 (d).

and TEOS (see Supporting Information Figure SI-10). Also, after addition of pure PTES in sample Ph-CMS 15 no phenyl groups were detected by Raman spectroscopy (see Supporting Information Figure SI-8). The observed results can be explained by taking into account the different oligosilicates resulting from hydrolysis and condensation of pure organosilane addition as compared to a mixture with TEOS during the formation mechanism of the functionalized outer layer (Figure 10).

In the case of pure functionalized triethoxysilanes, the oligosilicates resulting from hydrolysis and condensation have few or no free silanol groups, which are necessary for attachment and further condensation to the inorganic framework. DLS measurements confirm the bimodal particle size distribution in sample AP-CMS 11 due to the generation of such species (Figure 11).

While samples coated with an APTES/TEOS mixture showed no significant difference in particle diameter with respect to uncoated samples, addition of pure APTES resulted in small particles which are attributed to agglomerations of aminopropyl-functionalized oligosilicates as well as larger

(25) Frasc, J.; Lebeau, B.; Soulard, M.; Patarin, J.; Zana, R. *Langmuir* **2000**, *16*, 9049–9057.

(26) Zhao, X. S.; Lu, G. Q.; Millar, G. J. *Ind. Eng. Chem. Res.* **1996**, *35*, 2075–2090.

agglomerates of such oligosilicates with the CMS particles. In the case of PTES, the resulting oligomer agglomerations were too small to be recovered by centrifugation and thus were removed from the sample, thus resulting in unfunctionalized material. It should be noted that this behavior is only observed for late addition times, that is, after 30 min or more. Materials synthesized by addition of pure organosilanes during early stages of particle growth show no differences to samples prepared by addition of TEOS-containing mixtures, as excess TEOS is still present in the reaction mixture at early particle growth stages.

Conclusion

A versatile approach for the selective functionalization of mesoporous silica nanoparticles has been developed. By using an in situ co-condensation approach during the growth of the particles, functional groups can be completely dispersed inside the channels, concentrated in parts of the mesopores, or exclusively placed on the external surface, depending on the time of addition. In this way, several disadvantages associated with postsynthesis grafting can be avoided, such as the unwanted partial functionalization of the internal surface by diffusion of grafting reactants into the mesopores. Furthermore, the functional group density on the outer particle surface can be easily adjusted by variation of the organosilane-to-TEOS ratio.

The resulting nanoparticles are promising candidates for the generation of sophisticated multifunctional systems, for example, in drug delivery applications. External functionalization allows for the attachment of bulky groups and other nanoparticles without reducing pore volume and causing excessive pore blocking. Moreover, selective functionalization of the outer particle surface does not influence the interactions of guest molecules with the internal pore walls and diffusion of the guest molecules inside the mesopores, which is an important aspect in drug delivery. By alteration of the internal surface in subsequent functionalization steps, such as postsynthesis grafting, the generation of materials with tailor-made properties becomes possible for which interactions with the environment and with guest species can be completely controlled.

Acknowledgment. The authors thank Markus Döblinger (University of Munich) for performing scanning transmission electron microscopy. Financial support from the SFB 486 (DFG) and the NIM-cluster is gratefully acknowledged.

Supporting Information Available: Additional zeta potential curves, thermogravimetric data, nitrogen sorption data, Raman spectra, and mathematical derivations used in STEM analysis (PDF). This material is available free of charge via the Internet at <http://pubs.acs.org>.

CM801484R